Correlation between interatomic distances and the x-ray-absorption near-edge structure of single-crystal sapphire

J. M. Chen
Synchrotron Radiation Research Center, Hsinchu, 30077, Taiwan, Republic of China

J. K. Simons
Department of Chemistry, University of Wisconsin, Madison, Wisconsin 53706

K. H. Tan
Canadian Synchrotron Radiation Facility, 3731 Schneider Drive, Stoughton, Wisconsin 53589

R. A. Rosenberg
Argonne National Laboratory, Argonne, Illinois 60439
(Received 28 June 1993)

The high-resolution Al L-edge x-ray-absorption near-edge structure from single-crystal sapphire has been recorded by measuring the total-electron yield and x-ray-fluorescence yield with synchrotron radiation. The edge structures up to 11 eV from the absorption edge are assigned in terms of the transitions of Al $2p$ electrons to empty levels using molecular-orbital calculations. The post-edge features between 11 and 60 eV above the Al L_{23} absorption edge were found to correlate very well with the interatomic distances from the absorbing atom to its neighboring atoms as predicted by the multiple-scattering model.

I. INTRODUCTION

Single-crystal sapphire is a good insulator with a band gap about 9 eV.[1] It is chemically stable and remains transparent even after exposures to high doses of γ radiation and high-energy electron beams.[2] These properties have led to its use in technological applications including such electronic devices as hot-electron tunnel transistors. In addition, single-crystal Al_2O_3 is a model compound for chemisorption studies of oxygen on aluminum and the oxidation of aluminum metal.[3] For years, its electronic structure has been the subject of numerous experimental investigations.[4–14]

The Al L-edge absorption spectrum of single-crystal Al_2O_3 is rich in structure. Interpretation of its absorption features has been the topic of numerous theoretical studies.[15–19] The earliest information on the electronic energy levels of single-crystal Al_2O_3 is provided by self-consistent-field $X\alpha$ scattered-wave calculations on the $[AlO_6]^{-9}$ cluster by Tossell.[18] However, this calculation fails to give the total width of the occupied and unfilled states obtained from soft-x-ray emission (SXE),[4] x-ray-photoelectron spectroscopy, and electron yield measurements.[7–9] Band-structure calculations have also been performed using the semiempirical Mullikin-Rûdenberg method[15] and the tight-binding method.[16,17] These calculations give reasonable values for the widths of the conduction band and some of the more prominent features in the SXE spectrum. However, there are some difficulties in defining the absorption spectrum using these band models, since they neglect the presence of unoccupied Al $3d$ orbitals in the basis set. These states are known to hybridize with empty aluminum states of s- and p-orbital symmetry and contribute significantly to the conduction-band density of states.[18] By employing the complete-neglect-of-differential-overlap (CNDO) approximation on the $[AlO_6]^{-9}$ cluster, Balzarotti *et al.* provided a realistic picture of electronic energy levels of Al_2O_3 to interpret the edge structures up to 11 eV above the Al L_{23} absorption edge.[19] But, to date, both band-structure and molecular-orbital calculations have failed to describe the post-edge region ($\sim$10–50 eV above the edge).[19]

A more refined description of the post-edge structure of single-crystal Al_2O_3 can be accomplished by constructing multiple-scattering states. At present, no comprehensive theory is available for the interpretation of the entire range of Al L-edge x-ray-absorption near-edge structure (XANES) spectrum of single-crystal sapphire. In this study, we apply the multiple-scattering model of Bianconi and Natoli to correlate the post-edge features in the XANES spectrum with the interatomic distances.

II. EXPERIMENTS

These experiments were performed on the $6m$ toroidal grating monochromator (TGM) beamline at Synchrotron Radiation Center (SRC), University of Wisconsin–Madison, in an ultrahigh vacuum chamber at a pressure of 2×10^{-10} Torr.

The experimental details have been reported previously,[20] so only pertinent details will be given here. The total-electron yield (TEY) spectrum and x-ray-fluorescence yield (XFY) spectrum were measured by a simple microchannel plate (MCP) detector. The MCP

0163-1829/93/48(14)/10047(5)/$06.00

detector consists of a dual set of MCP's (25-mm diam) with three electrically isolated grids mounted in front of them. The MCP detector was located ~5 cm from the sample and oriented parallel to the sample surface. Photons were incident at an angle of 45° with respect to the sample normal. The samples were 1-mm-thick, 12-mm-diam single crystal (0001) sapphire disks purchased from Meller Optics, Inc., which were polished by the manufacturer to one microinch or better. After rinsing with methanol, the samples were mounted in the chamber. No further surface preparation was made. The reference beam intensity (I_0) was measured simultaneously with a 90% transmission Ni mesh. All measurements were normalized to I_0. The L_{23} absorption edge (73.15 eV and 72.72 eV) of an Al filter was used to calibrate the photon energy to within ±0.1 eV. The 6m TGM beamline was operated with 200-μm slits, which corresponds to a theoretical resolution of 0.25 eV at 100 eV.

III. RESULTS AND DISCUSSION

A. Low-energy region (< 11 eV above the edge)

The structure from threshold to 11 eV above threshold has been thoroughly discussed previously. In particular, O'Brien *et al.* have recently discussed the effects of intermediate couplings in the L_2 and L_3 core exciton[21] and compared theory and experiment for the other peaks near threshold.[4] For completeness, we will discuss pertinent aspects of the low-energy region in the following paragraphs.

The high-resolution Al L-edge TEY spectrum and XFY spectrum from single-crystal sapphire at 298 K in the 76–92 eV region is presented in Fig. 1. There is a pronounced doublet splitting of the Al L_2 and L_3 components (78.80 eV and 78.38 eV) and a few superimposed features (peaks b–f). Separation of the Al L_{23} edge components yields a spin-orbit splitting of 0.42±0.02 eV. This value agrees with the absorption results of Al by Codling and Madden[14], with the emission data of Al by Skinner,[22] and with theoretical splitting of 0.48 eV obtained from a Hartree-Fock calculation.

In Table I we list the energies of significant experimental peaks in the XANES spectrum of single-crystal Al_2O_3. The peak energies were determined by curve fitting the peaks to Gaussian functions after subtracting a polynomial background. The errors were determined from estimated uncertainties in the curve fitting. These peak positions agree very closely to the values from Ref. 19 and estimated from Refs. 7 and 13. The absorption features in the TEY and XFY spectra in Fig. 1 are similar, but are much better defined in the latter. In addition, it can be seen that the L_3 absorption peak to the below-edge background ratio is much enhanced in the XFY spectrum. This is due to the fact that the x-ray fluorescence is available only if there is an Al(2p) hole, so the x-ray emission is zero below the edge, and above the edge its probability is proportional to the photoionization cross section of the Al(2p) level. In Fig. 1, the length of the arrows located at 76 eV in each curve represents an increase of 20% of the signal level at 76 eV. For the TEY the strong peak at 78.8 eV is only 17% greater than the background level at 76 eV, while for XFY the peak is 200% greater. Furthermore, there is an increasing background in the TEY spectrum, which we believe is due to increased charging at energies above the Al L edge.

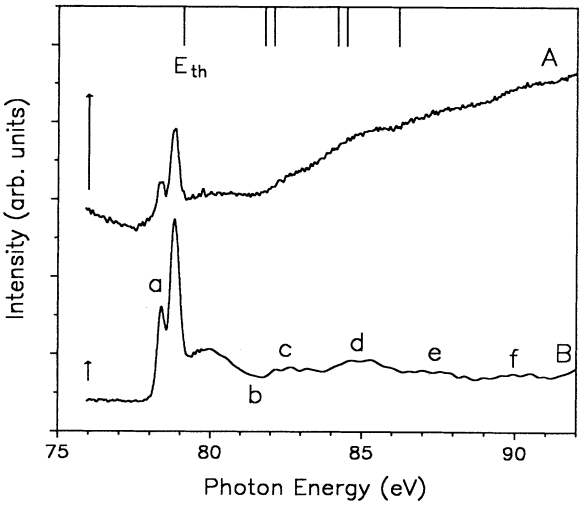

FIG. 1. Comparison of the electronic energy levels shown as vertical bars on the top of figure according to the calculations of Balzarotti *et al.*[19] with the present Al L-edge absorption spectra from single-crystal sapphire obtained using (a) TEY and (b) XFY. The length of the arrows at 76 eV represents an increase of 20% of the signal level at that energy.

As calculated from the x-ray-fluorescence spectrum shown in Fig. 1(b), the observed L_3/L_2 intensity ratio is 0.36, which is less than the statistical value of 2.[23] Onodera and Toyozawa showed in a model for the electronic transition $p^6 \rightarrow p^5 s$ in the alkali halides that the branching ratio is fairly sensitive to the electron-hole exchange energy.[23] When the core-hole spin-orbit interactions ε is much greater than the electron-hole exchange interaction Δ in the final state, jj coupling is obeyed. In jj coupling, the relative L_3/L_2 intensity for an excitation of the type $p^6 \rightarrow p^5 s$ will have the statistical value of 2/1. In the in-

TABLE I. Positions of the absorption peaks of Al L-edge XANES spectrum of single-crystal sapphire. The energies are expressed in eV.

	Present work	Ref. 7[a]	Ref. 13[a]	Ref. 19
a	78.38, 78.80	78.9	78.9	78.9
b	81.5±0.2	81.5	82.1	82.0
c	82.6±0.2	82.7	83.7	83.0
d	85.0±0.2	85.3	86.3	85.2
e	87.6±0.2	87.7	87.9	88.2
f	90.0±0.2	90.1	90.0	90.0
g	94.7±0.3	95.4	96.0	95.9
h	98.6±0.3	99.4	100.8	98.0
i	102.3±0.3			101.0
j	124.0±0.3			
k	128.6±0.3			

[a]Estimated from this reference.

termediate region ($0<\Delta<\varepsilon$), the branching ratio deviates considerably from 2/1 when the exchange energy increases. The statistical ratio gradually changes to the extreme intensity ratio of zero when the core-hole spin-orbit interaction is reduced to zero (*LS* coupling). This model now has been widely applied. Recently, this theory has been expanded to include crystal-field effects.[24,25] In addition, using the Onodera model, the exchange energy can be calculated according to the following equation:

$$I(L_3)/I(L_2)=\tan^2[\arctan 2^{1/2}-\tfrac{1}{2}\arctan 8^{1/2}\Delta/(3\varepsilon-\Delta)] \ . \quad (1)$$

Here, $\varepsilon=0.42$ eV. The obtained electron-hole exchange energy is 0.35 eV, which agrees closely to the value calculated from reflection spectrum of sapphire.[21]

Many theoretical studies in the past have concentrated on interpretation of the first few peaks (a–f) of the XANES spectrum of single-crystal sapphire.[15–19] Recently, Balzarotti *et al.* have performed CNDO calculations on the $[AlO_6]^{-9}$ molecule to explain the Al(2*p*) absorption spectrum of α-Al_2O_3.[19] The CNDO method has proven to be a valuable approximation for calculating the electronic energy levels of many solid materials.[26,27] It is therefore relevant to compare the present Al *L*-edge absorption features with energies predicted from the calculation of Balzarotti *et al.* The theoretical energy level positions are indicated as vertical bar shown on the top of Fig. 1. The value of the photoconduction threshold is 79.1 eV as determined in Ref. 21.

Since the main features of XANES of sapphire, such as *a*, *b*, *c*, *d*, etc., appear in SXE,[4] this indicates that they must be due to localized resonant excitations. As seen from Fig. 1, the two spin-orbital coupling pairs of the Al *L*-edge XANES spectrum lie in the band gap[1] (about 9 eV) and are therefore interpreted in terms of exciton absorption.[6] Similar structures have been observed in the vacuum ultraviolet (VUV) optical[1] and soft-x-ray-absorption spectra.[28] According to the calculation of Balzarotti *et al.*, the exciton peaks originate largely from Al 3*s* levels pulled down into the band gap from the bottom of the conduction band by the core-hole potential. The feature at position *b* has primarily Al 3*p* character, which is dipole forbidden and is therefore not observed. A corresponding pronounced maximum exists in the electron-yield Al *K*-edge spectrum of single-crystal Al_2O_3 (Ref. 7) and in the Al *K*-edge photoabsorption spectrum of γ-Al_2O_3.[29] The next structures, peaks *d*-*f*, are derived mainly from the Al 3*d* orbitals ($d_{x^2-y^2}$, d_{xy}, d_{x^2}, d_{xz}, and d_{yz}). However, the calculation of Balzarotti *et al.* fails to describe the structures corresponding to peaks *g*-*k* in Fig. 2.[19]

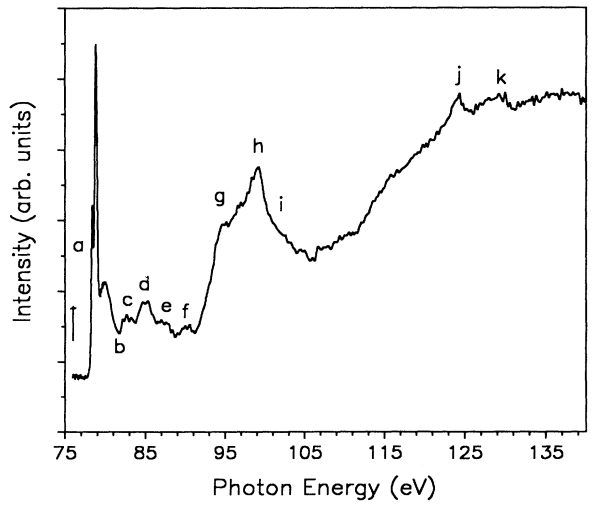

FIG. 2. Al *L*-edge x-ray-absorption near-edge structure from single-crystal sapphire in the energy range 76–140 eV obtained using XFY. The length of the arrows at 76 eV represents an increase of 20% of the signal level at that energy.

B. Interatomic distance correlation

Recently, many papers have pointed out that including multiple scattering effects is essential for interpreting the higher-energy post-edge structure in the XANES spectrum.[30,31] Using multiple scattering theory, Bianconi and Natoli have shown that the post-edge absorption features can be correlated with interatomic distances.[32] There was some initial success in the application of the model. For example, Bianconi *et al.* correlated the nearest-neighbor distance in a series of $3d^0$ compounds, including Ti^{+4}, V^{+5}, and Cr^{+6} (all tetrahedrally coordinated to oxygen) with a broad peak in the *K*-edge XANES spectrum of the metals.[33] Lytle, Greegor, and Panson correlated some of the transitions in the XANES region to the bond lengths in certain metal oxides.[34] In the case of NiO, they were able to identify and assign the Ni *K*-edge features to long-range interatomic distances up to the

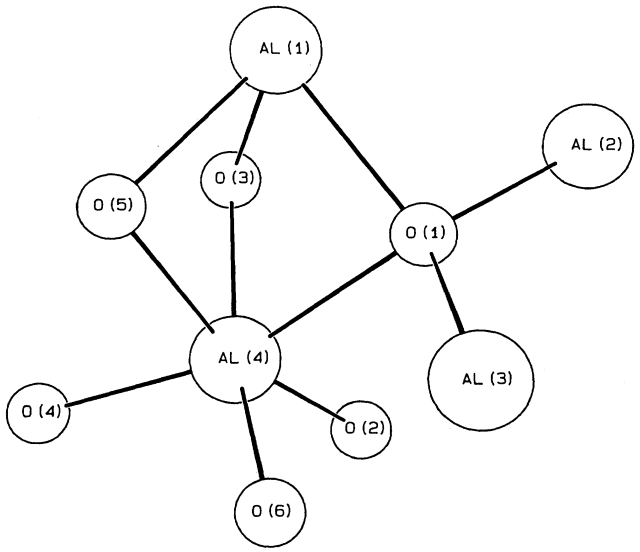

FIG. 3. The atomic structure in the unit cell of single-crystal sapphire. Each Al atom is surrounded six oxygen atoms, three [Al(4)-O(1), Al(4)-O(3), and Al(4)-O(5)] at a distance of 1.84 Å, and the other three [Al(4)-O(2), Al(4)-O(4), and Al(4)-O(6)] at a distance of 1.98 Å.

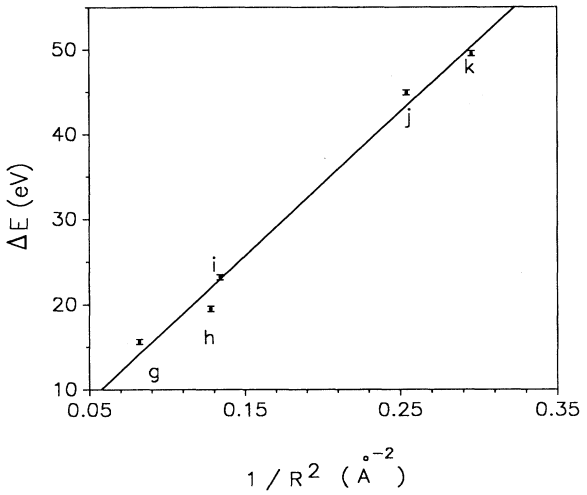

FIG. 4. Correlation plot between ΔE and $1/R^2$ for Al L-edge XANES of single-crystal sapphire.

fourth coordination sphere. Investigating the S L-edge XANES spectra of sulfide minerals, including ZnS, MoS_2, and PbS, Kasrai *et al.* were able to assign all the peaks between 10 and 45 eV above the edge to interatomic distances.[35] They have also successfully correlated the Cl L-edge XANES of alkali halides ($\sim$10–50 eV above the absorption edge) with interatomic distances.[36] There is now a growing number of empirical observations that support the peak energy-distance correlation.

It was shown by Natoli that the energy of an absorption peak above the photoconduction threshold is inversely proportional to the separation R, from the absorbing atom to a neighboring atom, according to the following equation:[32]

$$(E_p - E_{\text{th}})R^2 = \Delta E R^2 = C \ , \tag{2}$$

where E_p is the energy of the peak of interest, E_{th} is the photoconduction threshold energy, and C is the constant for absorbing material. It can be shown that for a free electron the value of C is 150.4 eV Å^2.[37] In practice C is determined by fitting the experimental data to Eq. (2).

Single-crystal sapphire has a rhombohedral symmetry (D^6_{3d} space-group symmetry) with two Al_2O_3 units in the primitive cell. The minimum $(Al_2O_3)_2$ cluster of sapphire is shown schematically in Fig. 3. In this structure, each Al atom has three nearest-neighbor atoms at a distance of 1.84 Å and three next-nearest atoms at a distance of 1.98 Å. Viewed from an oxygen site, it appears to be surrounded by four Al atoms, two at a distance of 1.84 Å and the other two at a distance of 1.98 Å. Calculated from crystal structure of Al_2O_3, the distances for Al(1)-Al(4), Al(2)-Al(4), and Al(3)-Al(4) are 2.73, 2.80, and 3.49 Å, respectively.[17]

It is obvious from the energy and distance relationship in Eq. (2) that the shorter the interatomic distance, the higher the energy of the corresponding absorption peak.

TABLE II. Peak assignments and interatomic distances for the post-edge peaks in the XANES spectrum of single-crystal sapphire.

Shell	Peak	E_p-E_{th}[a] (eV)	R (Å)[b] Calc.	R (Å) Present
R_1	k	49.5	1.84	1.85±0.01
R_2	j	44.9	1.98	1.94±0.01
R_3	i	23.2	2.73	2.70±0.02
R_4	h	19.5	2.80	2.95±0.02
R_5	g	15.6	3.49	3.30±0.03

[a]E_{th} is 79.1 eV determined in Ref. 21.
[b]Calculated from crystal structure according to Ref. 17.

After locating the peak corresponding to the first-nearest-neighbor shell in the region of 30–50 eV above the edge, the other peaks can be correlated sequentially.

A plot of ΔE against $1/R^2$, as shown in Fig. 4, reveals a linear correlation with an intercept of $\sim$0.28 eV. The value of C calculated from the slope of this plots is 169.4 eV Å^2. Deviation of the constant C from the free-electron value is related to changes in the phase shift during backscattering. In Table II, we summarize the results of the correlations and compare the derived distances with the experimental values. Looking at Fig. 4 and Table II, we notice that the correlation between the experimental and derived distances is within 0.04 Å for the first three peaks and 0.16 Å for the other two peaks. In addition, it can be seen from Fig. 2 that the intensity of peaks $g-i$ is stronger than that of peaks j and k. This is because the scattering between the Al atoms is greater than that between Al atoms and oxygen atoms.

IV. CONCLUSION

In this paper, we report the Al L-edge XANES spectra from single-crystal sapphire obtained using TEY and XFY. The signal-to-background of the XFY spectrum is enhanced compared to the TEY. This result shows that XFY measurement is a powerful method to measure the bulk extended x-ray-absorption fine structure (EXAFS) and XANES for structural information, especially for insulating sample. The experimental structures up to 11 eV from Al L_{23} absorption edge are interpreted in terms of the transition of electrons to empty levels of Al ion of predominant s, p, and d character according to the molecular-orbital calculations on the $[AlO_6]^{-9}$ cluster by Balzarotti *et al.*[19] The post-edge features between 11 and 60 eV above the Al L_{23} absorption edge correlate well with the interatomic distances as predicted by the multiple scattering model of Bianconi and Natoli.[32]

ACKNOWLEDGMENTS

We would like to thank the staff at the Synchrotron Radiation Center, University of Wisconsin–Madison for their technical support.

[1]E. T. Arakawa and M. W. Williams, J. Phys. Chem. Solids **29**, 735 (1968).
[2]S. M. Sze, *Physics of Semiconductors Devices* (Wiley, New York, 1969).
[3]D. Norman, S. Brenann, R. Jaeger, and J. Stöhr, Surf. Sci. **105**, L297 (1981).
[4]W. L. O'Brien, J. Jia, Q. Y. Dongg, T. A. Callcott, J. E. Rubensson, D. L. Mueller, and D. L. Ederer, Nucl. Instrum. Methods B **56/57**, 320 (1991).
[5]T. Tomiki, T. Futemma, H. Kato, T. Miyahara, Y. Aiura, H. Fukutani, and T. Shikenbrau, J. Phys. Soc. Jpn. **58**, 1486 (1988).
[6]A. Balzarotti, F. Antonangeli, R. Girlanda, and G. Martino, Solid State Commun. **44**, 275 (1982).
[7]I. A. Brytov and Yu. N. Romaschenko, Fiz. Tverd. Tela (Leningrad) **20**, 664 (1978) [Sov. Phys. Solid State **20**, 384 (1978)].
[8]S. P. Kowalczyk, F. R. McFeely, L. Ley, V. T. Gritsyna, and D. A. Shirley, Solid State Commun. **23**, 161 (1977).
[9]A. Balzarotti and A. Bianconi, Phys. Status Solidi B **76**, 689 (1976).
[10]V. A. Fomichev, Fiz. Tverd. Tela (Leningrad) **8**, 2892 (1966) [Sov. Phys. Solid State **8**, 2312 (1967)].
[11]N. Swanson and C. J. Powell, Phys. Rev. **167**, 592 (1968).
[12]A. Balzarotti, A. Bianconi, E. Burattini, M. Grandolfo, R. Habel, and M. Piacentini, Phys. Status Solidi **63**, 77 (1974).
[13]A. Bianconi, Surf. Sci. **89**, 41 (1979).
[14]K. Codling and R. P. Madden, Phys. Rev. **167**, 587 (1968).
[15]R. A. Evarestov, A. N. Ermoshkin, and V. A. Lovchikov, Phys. Status Solidi B **99**, 387 (1980).
[16]S. Ciraci and I. P. Barta, Phys. Rev. B **28**, 982 (1983).
[17]I. P. Barta, J. Phys. C **15**, 5399 (1982)
[18]J. A. Tossell, J. Phys. Chem. Solids **36**, 1273 (1975).
[19]A. Balzarotti, F. Antonangeli, R. Girlanda, and G. Martino, Phys. Rev. B **29**, 5903 (1984).
[20]R. A. Rosenberg, J. K. Simons, S. P. Frigo, and J. M. Chen, Rev. Sci. Instrum. **63**, 2193 (1992).
[21]W. L. O'Brien, J. Jia, Q. Y. Dong, T. A. Callcott, J. E. Rubensson, D. L. Mueller, and D. L. Ederer, Phys. Rev. B **44**, 1013 (1991).
[22]H. W. B. Skinner, Philos. Trans. R. Soc. London, Ser. A **239**, 95 (1940).
[23]Y. Onodera and Y. Toyozawa, J. Phys. Soc. Jpn. **22**, 833 (1967).
[24]G. van der Laan and B. T. Thole, Phys. Rev. Lett. **60**, 1977 (1988).
[25]F. M. F. de Groot, J. C. Fuggle, B. T. Thole, and G. A. Sawatzky, Phys. Rev. B, **42**, 5459 (1990).
[26]Taguena-Martinez, L. E. Sansores, and E. A. Cetina, Phys. Rev. B **27**, 2435 (1983).
[27]H. Haberlandt and F. Ritschl, Phys. Status Solidi B **100**, 503 (1980).
[28]K. H. Lee and J. H. Crawford, Phys. Rev. B **15**, 4065 (1977).
[29]C. Senemaud and M. T. Costa Lima, J. Phys. Chem. Solids **37**, 83 (1976).
[30]J. Garcia, M. Benfatto, C. R. Natoli, A. Bianconi, I. Davoli, and A. Marcelli, Solid State Commun. **58**, 595 (1986).
[31]A. Bianconi, A. Di Cicco, N. V. Pavel, M. Benfatto, A. Marcelli, C. R. Natoli, P. Pianetta, and J. Woicik, Phys. Rev. B **36**, 6426 (1987).
[32]C. R. Natoli, in *EXAFS and Near Edge Structure,* Springer Series in Chemical Physics Vol. 27, edited by A. Bianconi, L. Incoccia, and S. Stipcich (Springer, Berlin, 1983), p. 43; in *EXAFS and Near Edge Structure III,* edited by K. O. Hodgson, B. Hedman, and J. E. Penner-Hahn (Springer-Verlag, Berlin, 1984), p. 38.
[33]A. Bianconi, E. Fritsch, G. Calas, and J. Petiau, Phys. Rev. B **32**, 4292 (1985).
[34]F. W. Lytle, R. B. Greegor, and A. J. Panson, Phys. Rev. B **37**, 1550 (1988).
[35]M. Kasrai, M. E. Fleet, T. K. Sham, G. M. Bancroft, K. H. Tan, and J. R. Brown, Solid State Commun. **68**, 507 (1988).
[36]M. Kasrai, M. E. Fleet, G. M. Bancroft, K. H. Tan, and J. M. Chen, Phys. Rev. B **43**, 1763 (1991).
[37]J. S. Tse, J. Chem. Phys. **89**, 920 (1988).